Inductance and Quality-Factor Evaluation of Planar Lumped Inductors in a Multilayer Configuration

Samir F. Mahmoud and Eric Beyne

***Abstract*—Integral representations for the self and mutual inductance of planar loops on a multilayered structure are derived. The integrals are of the Sommerfeld type and can be easily evaluated under the quasi-static approximation which is validated by the small dimensions relative to a wavelength. Enhancement of loop inductance by inclusion of a magnetic layer is investigated. It is shown that such a layer can increase the inductance by a percentage which has the upper limit of $[(\mu_r-1)/(\mu_r+1)]\times 100\%$, where μ_r is the relative permeability of the layer. A study is also made on the inductor quality factor (Q) as affected by losses caused by finite electrical conductivity of the magnetic layer and the underlying substrate.**

I. Introduction

IT IS WELL KNOWN that lumped elements in microwave planar circuits can potentially reduce a circuit's physical size. Several lumped inductor and capacitor configurations have been proposed and utilized in active and passive circuit designs [1]–[6]. Although simple formulas have been proposed for analysis and design of these elements (e.g. [7]–[9]), exact prediction of inductance or capacitance of lumped elements on a multilayer structure still poses challenging problems if the effect of the underlying structure is to be fully accounted for.

Simple formulas have been provided by Greenhouse [7], based on earlier work of Grover [8] and Terman [9], to compute the self-inductance of a straight strip in terms of its width and thickness, and the mutual inductance between two straight parallel strips separated by a given spacing. Other formulas have been presented more recently by Pettenpaul *et al*. [10] who consider both rectangular, as well as circular, multiturn coils. It is worth noting that the inductance formulas presented in the above papers do not account for reflections from the multilayer structure underneath, except for the ground plane. This may be acceptable if there is no magnetic layer involved. Such a layer will have appreciable effect on the value of inductance. In this paper, a method is presented for deriving self-inductances of printed coils or rings taking full account of the multilayers beneath them. This method is based on expanding the electromagnetic field due to the ring current into a spectrum of plane waves, which are reflected and transmitted at the lower multilayer structure. An integral form of the Sommerfeld type is thus derived for the flux linkage with the ring and, therefore, the self-inductance of the ring. As a special case, the effect of a magnetic slab of a given thickness within the multilayer structure on the ring inductance is studied. One can also find the effect of losses due to the layers' conductivities on the measured ring resistance or the ring quality factor (Q). A similar method had been presented earlier by Wait and Spies [11], to derive the input impedance of a loop above a lossy earth.

Manuscript received April 24, 1996; revised February 28, 1997.

S. F. Mahmoud is with the ECE Department, Kuwait University, 13060 Safat, Kuwait.

E. Beyne is with IMEC, B-3001 Leuven, Belgium.

Publisher Item Identifier S 0018-9480(97)03914-8.

II. Derivation of Primary Inductance

First consider a ring strip with a mean radius a and width w, where $w \ll a$, lying in the plane $z = 0$, as demonstrated by Fig. 1(a). It is required to derive the self-inductance of the ring strip in free space. Consider next the case where the ring is situated on the top of a layered horizontally stratified medium as depicted in Fig. 1(b).

Referring to Fig. 1(a), adopt a cylindrical coordinate system (r, φ, z) and assume an electric surface current density J A/m flowing in the ϕ direction and harmonically varying with time as $\exp(j\omega t)$ and ω being the radian frequency. For a ϕ independent current, J can be expressed by

$$J(r) = \begin{cases} (I/w)f(r), & a - w/2 \le r \le a + w/2 \\ 0, & \text{otherwise} \end{cases} \tag{1}$$

where I is the total current (ampere) and $f(r)$ is the radial current distribution such that $\int f(r)\,dr = w$ over the ring. Strictly speaking, $f(r)$ should be obtained from the solution of a boundary value problem requiring the vanishing of the tangential electric field to the ring's surface. An acceptable solution for $f(r)$ on a strip line has been found [12] to be

$$f(r) = (w/\pi)[(w/2)^2 - (r-a)^2]^{-1/2} \tag{1a}$$

which takes into account the edge effect. This form of current distribution shall be adopted in what follows. As a step toward derivation of the electromagnetic fields produced by this current, $J(r)$ is recast into a continuous spectrum of cylindrical waves as

$$J(r) = I \int_o^\infty S(\lambda) J_1(\lambda r) \lambda \, d\lambda \tag{2}$$

where $J_1(\cdot)$ is the first-order Bessel function. Equating (1) and (2), and using the Bessel transform relation, one gets

$$S(\lambda) = (1/w) \int_{a-w/2}^{a+w/2} f(r) J_1(\lambda r) r \, dr \tag{3a}$$

$$\cong (a/w) J_1(\lambda a) \int_{a-w/2}^{a+w/2} f(r) \frac{J_1(\lambda r)}{J_1(\lambda a)} \, dr. \tag{3b}$$

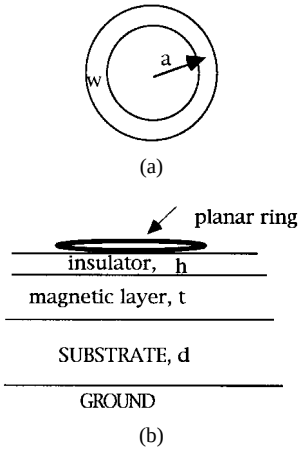

Fig. 1. Problem geometry. (a) Single planar ring in the plane $z = 0$, mean radius a, and width w. (b) Inductor ring on a multilayer structure.

Since $(r - a) \leq w/2 \leq a$ in the above integral, the ratio of the Bessel functions inside the integrand can be approximated by using the large argument approximation for these functions leading to $J_1(\lambda r)/J_1(\lambda r) \approx \cos(\lambda(r-a))$. This approximation turns out to be a very good one for λ in the order of $1/a$ or greater, which covers the significant range of λ as will be further discussed below. Performing the integration in (3b), one gets

$$S(\lambda) \cong aJ_1(\lambda a)J_o(\lambda w/2). \tag{3c}$$

The electromagnetic fields associated with the current can be expressed in terms of a z-oriented vector electric potential [13], which satisfies the wave equation in air and, therefore, is given by

$$F(r,z) = \int_o^\infty A(\lambda)J_o(\lambda r)\exp(-u_o|z|) \tag{4}$$

where

$$u_o = (\lambda^2 - k_o^2)^{1/2} \quad \text{and} \quad k_o = \omega(\mu_o\varepsilon_o)^{1/2}.$$

Noting that the magnetic field component $H_r(r,0^+) = J/2$ from Ampere's law, (2), (3c), (4), and the relation $H_r = \partial^2 F/\partial r\partial z$ are used to find $A(\lambda)$ and, therefore, $F(r,z)$ is now rewritten in terms of the current as

$$F(r,z) = \frac{Ia}{2}\int_o^\infty \frac{1}{u_o}J_1(\lambda a)J_o(\lambda w/2)J_o(\lambda r)e^{-u_o|z|}\,d\lambda. \tag{5}$$

The vertical magnetic field $H_z(r,z)$ is obtained from $F(r,z)$ through a well-known relation [13] leading to

$$H_z(r,z) = \frac{Ia}{2}\int_o^\infty \frac{\lambda^2}{u_o}J_1(\lambda a)J_o(\lambda w/2)J_o(\lambda r)e^{-u_o|z|}\,d\lambda. \tag{6}$$

Now, one is in a position to derive the magnetic flux linkage with the ring from which the primary inductance L_p is obtained in free space; namely

$$\begin{aligned} L_p &= \mu_o\int_o^a H_z(r,o)2\pi r\,dr/I \\ &= \pi\mu_o a^2\int_o^\infty \frac{\lambda}{u_o}J_1^2(\lambda a)J_o(\lambda w/2)\partial\lambda \end{aligned} \tag{7}$$

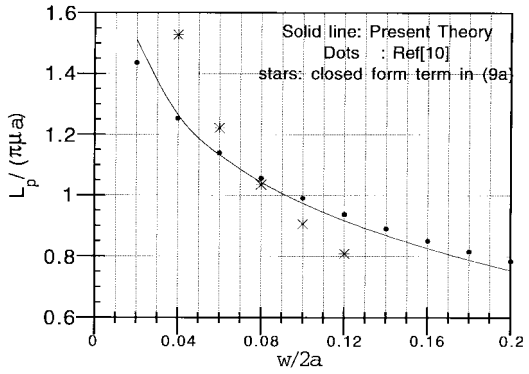

Fig. 2. Normalized inductance of a single ring inductor in free space versus $\overline{w} = w/2a$, as obtained by (9). Comparison with results based on [10] is shown by dots. The stars give the closed form term $(1-\overline{w})/\pi\sqrt{\overline{w}}$.

where the identity [14]

$$\int_o^a J_o(\lambda r)r\,dr = a^2J_1(\lambda a)/\lambda a$$

has been utilized. Formula (7) is an integral expression for the ring self-inductance. It may be re-expressed in dimensionless quantities by using the substitution $x = \lambda a$ and $\overline{w} = w/2a$, leading to

$$L_p/(\pi\mu_o a) = \int_o^\infty \frac{x}{(x^2 - k_o^2a^2)^{1/2}}J_1^2(x)J_o(x\overline{w})\,dx. \tag{8}$$

It is noticed that the square-root term will be imaginary in the range $o < x < 1$, thus rendering L complex. The imaginary part of L accounts for the radiation resistance of the ring. When the ring radius is much less than the free-space wavelength, i.e., $k_0a \ll 1$, which is usually the case of interest, this resistance is negligible. Furthermore, one can neglect k_0a relative to x since the bulk of the integral in (8) comes from the range of $x \geq 1$. Therefore, (8) can be rewritten in the form

$$L_p/(\pi\mu_o a) = \int_o^\infty J_1^2(x)J_o(x\overline{w})\,dx. \tag{9}$$

Obviously (9) can be obtained by using the quasi-static approximation right from the outset, on account of the small ring dimensions relative to a wavelength. For instance, a ring of mean radius $a = 250\ \mu$m is one hundredth of a wavelength at 12 GHz, which validates a quasi-static approach.

It should be noted that as w tends to zero in (9), the integral will diverge, indicating that as expected, the inductance of a zero-thickness ring is infinite. For the purpose of computing L_p in (9), the integral is recast into a closed-form term plus a correction term; the details of which are given in the Appendix-A. Thus

$$L_p/(\pi\mu_o a) = \frac{1-\overline{w}}{\pi\sqrt{\overline{w}}} + \int_0^\infty [T(x) - T_\infty(x)]\,dx \tag{9a}$$

where $T_\infty(x)$ is an asymptotic form of $T(x)$ as given in the Appendix-A.

Numerical values of $L_p/(\pi\mu_o a)$ for a single loop, as given by (9), is plotted versus $\overline{w}$ in Fig. 2, a solid curve and comparison is made with results computed from a formula in [10, eq. (10)]. Good agreement is found between this paper's

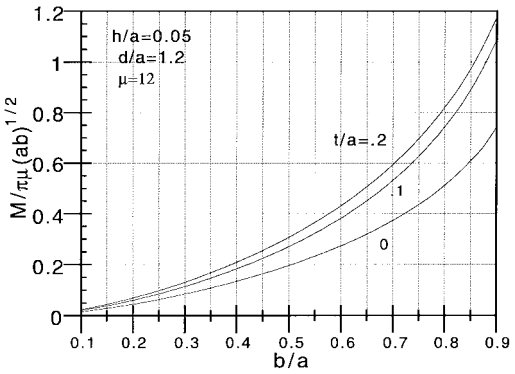

Fig. 3. Normalized mutual inductance between two rings of mean radii a, b in free space $(t/a = 0)$ versus b/a as given by (8), and in the presence of a magnetic slab of thickness t.

approach and that in [10]. It is worth mentioning that the closed-form term on the right-hand side (RHS) of (9a) can stand alone as a rough approximation with less than 10% error in the narrow range $0.6 \leq \overline{w} \leq 0.1$, as shown by stars in Fig. 2. The integral term in (9a) changes its sign from negative to positive as $\overline{w}$ increases and passes by ≈ 0.08.

The same formulation given above can be adapted to obtain the mutual inductance M between two concentric rings of mean radii a and b with, say, $b < a$. With $w \ll a, b$ and $b - a$, it can now be assumed that the ring currents are concentrated at the mean radii of the rings. Therefore, (1)–(9) applies with the exceptions that w is set equal to zero and the integration limits in (7) change to become from zero to b. Thus $M(a,b)$ is given by

$$M(a,b) = \pi\mu_o b \int_o^\infty J_1(x) J_1(xb/a)\, dx. \tag{10}$$

Fortunately, this integral has a standard form [14, Ch. 11] and, hence, a closed form for $M(a,b)$ is

$$M(a,b)/(\pi\mu_o\sqrt{ab}) = \tfrac{1}{2}\,(b/a)^{3/2} F[\tfrac{3}{2}, \tfrac{1}{2}; 2, (b/a)^2] \tag{11}$$

where $F(x, y; z, t)$ is the hypergeometric function defined in [14, Ch. 15]. Numerical values of the left-hand side (LHS) of (11) versus (b/a) are shown by the curve labeled 0 in Fig 3. It is worth noting that $M(a,b)$ can also be expressed in terms of the complete elliptic functions [15] as

$$M(a,b)/(\pi\mu_o\sqrt{ab}) = (2(a/b)^{1/2}/\pi)[K(b/a) - E(b/a)] \tag{11a}$$

where $E(x)$ and $K(x)$ are the complete elliptic integrals as defined in [14, ch. 17].

III. Effect of the Multilayer Structure

A ring is now considered, which is situated on the top of a layered planar structure consisting of an insulating layer over a magnetic slab on a metal-packed substrate as depicted in Fig. 1(b). The cylindrical wave expansion of the primary vector potential F in (5) allows the inclusion of reflections from the planar structure in a straightforward manner. Namely, assuming $\Gamma(\lambda)$ to be the Fresnel reflection coefficient of the cylindrical wavelet $J_o(\lambda r)\exp(u_o z)$ incident on the planar structure, $F(r,z)$ in the presence of the lower half space becomes

$$F(r,z) = \frac{Ia}{2}\int_o^\infty \frac{1}{u_o} J_1(\lambda a) J_o(\lambda w/2) J_o(\lambda r)\{1 + \Gamma(\lambda)\} \cdot \exp(-u_o z). \tag{12}$$

Following the same steps leading to (9), one gets the ring inductance in the presence of the planar structure as

$$L/(\pi\mu_o a) = \int_o^\infty J_1^2(x) J_o(x\overline{w})\{1 + \Gamma(x)\}\, dx \tag{13}$$

where $x = \lambda a$ as before. $\Gamma(x)$ is derived in the Appendix using a transmission-line analogy in the vertical direction. It is shown that this is also a function of the bulk complex wavenumbers k_i, k_m, k_s in the insulator, the magnetic layer, and the substrate, respectively. If all wavenumbers are neglected relative to the transverse wavenumber λ, one is effectively using a quasi-static analysis, which leads to real values for the inductance L. This is justifiable in view of the small relevant dimensions in relation to a wavelength and, therefore, the quasi-static approximation is accurate enough for computing the inductance. Under this approximation, the conduction and displacement currents in the layers are totally neglected and the only important material parameter is the relative permeability of the magnetic layer. However, if one is interested in accounting for losses in the layered medium, then a full-wave analysis has to be pursued, i.e., conduction and displacement currents in the layers should be taken into account. Such losses are made of power loss due to the layers' conductivities and trapped surface waves traveling sideways within the layers.

Computation of L in (13) is performed by dividing the integration into a primary inductance L_p plus a secondary inductance L_s; the latter accounts for $\Gamma(x)$. The integration for L_s can be evaluated numerically since $\Gamma(x)$ includes an exponentially decaying factor that assures fast convergence of the integral (see Appendix-B).

IV. Numerical Examples

A. Grounded Substrate Under an Insulating Layer

First the multilayer structure is considered to consist of an insulating layer of thickness h above a grounded substrate of thickness d. Under the quasi-static approximation, the insulating and the substrate layers appear transparent and the inductance is only affected by the ground plane. In this case, the Fresnel reflection coefficient is simply $\Gamma(\lambda) = -\exp(-\lambda(d+h))$, where h and d are the insulator and the substrate thicknesses. The ratio L_s/L_p is plotted versus $(d+h)/a$; a being the mean coil radius in Fig. 4. It is shown that L_s/L_p is small, unless the ground plane is too close to the coil in relation to its radius. If the substrate losses caused by finite substrate conductivity are to be accounted for, one should abandon the quasi-static approximation and use the exact formula (A6) along with (A8) for $\Gamma(x)$. For a silicon substrate, the relative permittivity is taken to equal 11.7 and the loss tangent $\tan(\delta s)$ is considered as a variable. Formula

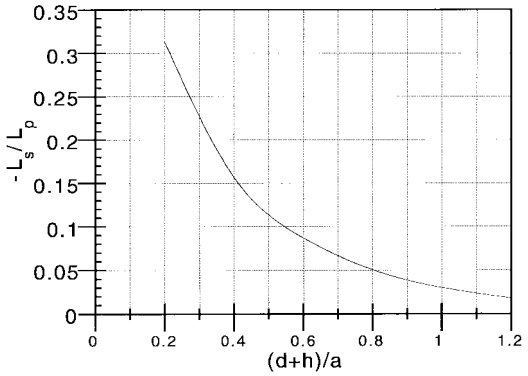

Fig. 4. The ratio $-L_s/L_p; L_s$ is caused by a grounded substrate of thickness d under an insulating layer of thickness h, versus $(d+h)/a; a$ being the ring mean radius. Quasi-static approximation is used.

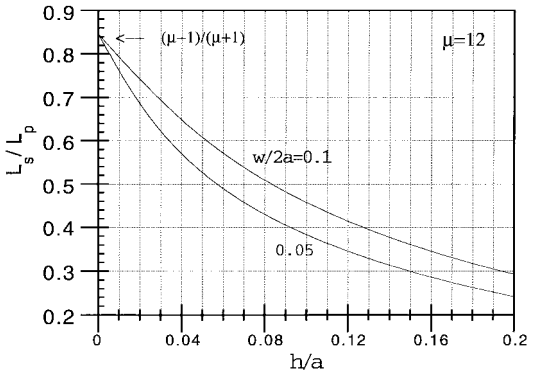

Fig. 6. The ratio $L_s/L_p\%$ of a single ring due to a magnetic half space at a depth h below the ring. $\mu_r = 12$.

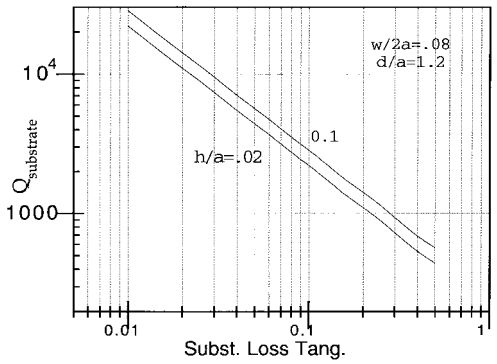

Fig. 5. The ring inductor Q due to substrate losses versus substrate loss tangent $(\tan \delta_s)$. Relative permittivity of substrate = 11.7 and the frequency is such that $k_o a = .0942$.

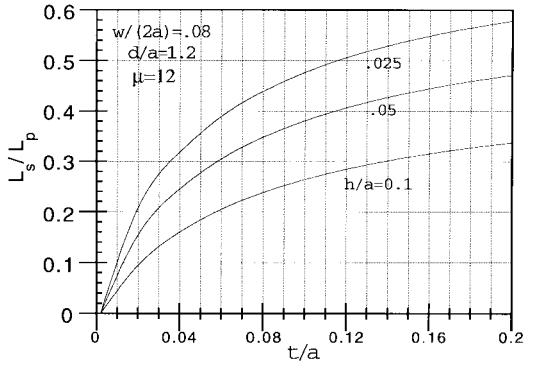

Fig. 7. The ratio L_s/L_p of a single ring on the multilayer structure of Fig. 1(b) versus the magnetic layer thickness with h/a as a parameter. $\mu_r = 12$.

(13) will now render complex values for L, the interpretation of which is that the imaginary part times ω is the part of the coil resistance as contributed by the substrate losses. A Q, $Q_{\text{substrate}}$, may be defined as the real part to the imaginary part of L. This is plotted versus $\tan(\delta s)$ in Fig. 5. The high values of Q shown signify low substrate losses and, therefore, the overall Q of the coil is not greatly affected by these losses. The latter is determined by all the losses, including the ohmic resistance of the ring, which is dominant. A full account of the ohmic resistance of printed conductors is found in [10].

B. A Multilayer Structure Containing a Magnetic Layer

Next, the effect of inclusion of a magnetic layer as depicted in Fig. 1(b) is studied. Under the quasi-static approximation, the electric conduction and displacement currents are neglected everywhere, so the reflection coefficient becomes a function of only λ, μ_r; the relative permeability of the magnetic slab and the geometrical dimensions as given by (A6) and (A7). Notably, in the limit $x \equiv \lambda a \gg 1$, [see (A10)]

$$\Gamma(x) \to [\mu_r - 1]/[\mu_r + 1] \exp(-2x\overline{h}) \tag{14}$$

where $\overline{h} = h/a$. In order to obtain an upper limit for L_s/L_p due to the presence of the magnetic layer, a hypothetical situation is considered in which this layer extends to fill the lower half space; i.e., $t \to \infty$. In this case, $\Gamma(x)$ is given exactly by (14). Therefore, the percentage L_s/L_p is bounded by $[\mu_r - 1]/[\mu_r + 1] \times 100\%$, which occurs at $h = 0$. Computation of that percentage as a function of h/a is performed, with the results plotted in Fig. 6. It is seen that the L_s/L_p drops monotonically with increased h/a; hence, the upper bound of the percentage increase of inductance due to a magnetic slab is a sensitive function of the insulating layer thickness. The effect of thickness of the magnetic slab is now studied by plotting L_s/L_p versus t/a, with h/a taken as a parameter in Fig. 7. As expected, as t/a increases, the L_s/L_p approaches its upper bound given in Fig. 6 for a given h/a.

The mutual inductance between two coaxial rings of mean radii a and b is also increased with the magnetic slab thickness. This is shown numerically in Fig. 3, in which $M(a,b)$ is plotted, versus b/a with t/a taken as a parameter and fixed h and d.

Finally, the conduction currents in the magnetic slab and substrate are accounted for by plotting the single ring Q_m (due to multilayer losses) versus frequency in gigahertz for typical dimensions where $a = 250\,\mu$m and other dimensions given in the Fig. 8 caption. The magnetic layer conductivity σ_m and h/a are taken as parameters. Here Q_m is defined as the real part of L to the imaginary part of L as caused by the magnetic slab and substrate conductivities. It is seen that Q_m increases inversely with h/a and is reduced with higher frequency and higher conductivity. This is so because as these two parameters increase, the magnetic slab thickness becomes a higher fraction of the skin depth δ. For instance, for $\sigma_m = 5$

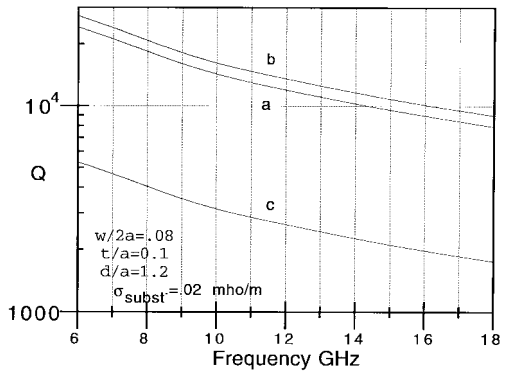

Fig. 8. The ring Q Q_{ms} due to losses in the magnetic layer and substrate versus frequency. $a = 25\,\mu\text{m}, t/a = 0.1, d/a = 1.2, \varepsilon_s = 11.7\varepsilon_o, \sigma_{\text{substrate}} = 0.2$ mho/m, $\mu_r = 12$. Curve (a): $\sigma_m = 1$ mho/m, $h/a = 0.02$, curve (b): $\sigma_m = 1$ mho/h, $h/a = 0.1$, and curve (c): $\sigma_m = 5$ mho/m, $h/a = 0.02$.

mho/m, and for $\mu_r = 12$, $t = 25\,\mu_m$, the skin depth $\delta \cong 28$ mm and $t/\delta \sim 0.9 \times 10^{-3}$ at 6 GHz and $t/\delta = 1.53 \times 10^{-3}$ at 18 GHz.

V. Conclusion

Integral Sommerfeld-type forms have been derived for the self and mutual inductances of planar rings on a multilayer structure with full account of reflections from, and transmission into, the multilayer medium. For ring dimensions which are very small, relative to the operating wavelength, a quasi-static approach renders accurate values of inductances. However, a full-wave analysis is needed if the substrate and/or the magnetic layer losses and their effect on the Q are to be accounted for. The introduction of a magnetic layer within the multilayer structure is shown to cause an increase of inductance—the upper limit of which is given by $[(\mu_r - 1)/(\mu_r + 1)] \times 100\%$, but the actual increase is a function of the insulator thickness h and the magnetic-layer thickness t, relative to the mean ring radius a. Ohmic losses in the magnetic layer remain small as long as the thickness is much less than a skin depth in the magnetic layer medium.

Appendix

A. Evaluation of (9)

Integration (9) can be recast into the following form:

$$L/(\pi\mu_o a) = \int_o^\infty T(x)\,dx = \int_o^\infty [T(x) - T_\infty(x)]\,dx + \int_o^\infty T_\infty(x)\,dx \tag{A1}$$

where $T(x) = J_1^2(x)J_o(x\overline{w})$ and $T_\infty(x)$ is an asymptotic form of $T(x)$ valid for $x \to \infty$

$$T_\infty(x) = \frac{J_1(x)}{x}\frac{2}{\pi\sqrt{\overline{w}}}\sin(x - \pi/4)\cos(x\overline{w} - \pi/4) = \frac{J_1(x)}{x}\frac{1}{\pi\sqrt{\overline{w}}}[\sin x(1 - \overline{w}) - \cos x(1 + \overline{w})] \tag{A2}$$

where the first term in the asymptotic expressions for each of $J_o(x)$ and $J_1(x)$ have been used.

It turns out that the integration of $T_\infty(x)$ in (A1) can be obtained in closed form as

$$\int_0^\infty T_\infty(x)\,dx = \frac{1 - \overline{w}}{\pi\sqrt{\overline{w}}}. \tag{A3}$$

where the following identities have been used [14, eq. (11.4.35), (11.4.36)]:

$$\int_o^\infty [J_1(px)/x]\sin(qx)\,dx = q/p, \qquad \text{for } 0 \le q \le p$$
$$\int_o^\infty [J_1(px)/x]\cos(qx)\,dx = 0, \qquad \text{for } q \ge p \ge 0$$

The other integral on the RHS of (A1) can be obtained numerically since the integrand approaches zero at sufficiently large x.

B. Fresnel Reflection Coefficient $\Gamma(\lambda)$

Under the quasi-static approximation, the bulk wavenumbers in each layer are neglected, relative to the transverse wavenumber λ. Hence, waves vary as $J_o(\lambda r)e^{\pm\lambda z}$ in each layer. The transverse impedance in each layer (considered as a transmission line along z) is $j\omega\mu/\lambda$; μ being equal to μ_o, except inside the magnetic layer where $\mu = \mu_o\mu_r$. With a perfectly conducting ground, the Fresnel reflection coefficient as seen at the top of the multilayer medium is

$$\Gamma(\lambda) = \exp(-2\lambda h)\Gamma'(\lambda) \tag{A6}$$
$$\Gamma'(\lambda) = \frac{(\mu_r^2 - 1)\tanh(\lambda t) + p(\tanh\lambda t - \mu_r)}{(\mu_r^2 + 1)\tanh(\lambda t) + 2\mu_r - p(\tanh\lambda t + \mu_r)} \tag{A7}$$

with $p = 1 - \tanh(\lambda d)$.

Next, if the wavenumbers in the substrate and the magnetic layer are not neglected, the transverse impedances in these layers become $j\omega\mu_o/u_s$ and $j\omega\mu_o/u_m$, respectively, where

$$u_s = (\lambda^2 - \omega^2\mu_o\varepsilon_s + j\omega\mu_o\sigma_s)^{1/2}$$
$$u_m = (\lambda^2 - \omega^2\mu_o\varepsilon_m + j\omega\mu\sigma_m)^{1/2}.$$

The Fresnel reflection coefficient is given by (A6) with

$$\Gamma'(\lambda) = \frac{\mu_r(\lambda T_s - u_s) + T_m(\mu_r^2\lambda u_s/u_m - u_m T_s)}{\mu_r(\lambda T_s + u_s) + T_m(\mu_r^2\lambda u_s/u_m + u_m T_s)}$$

where

$$T_s\tanh(u_s d) \quad \text{and} \quad T_m = \tanh(u_m t). \tag{A8}$$

Note that as

$$\lambda \to \infty \Gamma' \to \frac{(\mu_r - 1)}{\mu_r + 1}. \tag{A9}$$

Hence,

$$\Gamma(\lambda)_{\lambda\to\infty} = \frac{\mu_r - 1}{\mu_r + 1}\exp(-2\lambda h). \tag{A10}$$

ACKNOWLEDGMENT

The authors wish to thank Prof. J. R. Wait for his critical reading of an earlier version of this paper and for his enlightening comments. S. Mahmoud wishes to acknowledge the research administration of Kuwait University for providing the computing facilities needed for this paper.

REFERENCES

[1] D. A. Daly, S. P. Knight, M. Caulton, and R. Ekholdt, "Lumped elements in microwave integrated circuits," *IEEE Trans. Microwave Theory Tech.*, vol. MTT-15, pp. 713–721, Dec. 1967.
[2] M. Caulton, B. Hershenov, S. P. Knight, and R. DeBrecht, "Hybrid integrated lumped element microwave amplifiers," *IEEE Trans. Electron Devices*, vol. ED-15, pp. 459–566, July 1968.
[3] _____, "Status of lumped elements in microwave integrated circuits: Present and future," *IEEE Trans. Microwave Theory Tech.*, vol. MTT-19, pp. 588–599, July 1971.
[4] C. S. Atchison, S. Collin, R. Davies, I. D. Higgins, S. r. Longley, B. H. Newton, J. F. Wells, and J. C. Williams, "Lumped-circuit elements at microwave frequencies," *IEEE Trans. Microwave Theory Tech.*, vol. MTT-19, pp. 928–937, Dec. 1971.
[5] M. Ingalls and G. Kent, "Monolithic capacitors as transmission lines," *IEEE Trans. Microwave Theory Tech.*, vol. MTT-35, pp. 964–970, Nov. 1987.
[6] R. G. Arnold and D. J. Pedder, "Microwave characterization of microstrip lines and spiral inductors in MCM-D technology," *IEEE Trans. Comp., Hybrids, Manufact. Technol.*, vol. 15, pp. 1038–1045, Dec. 1992.
[7] H. M. Greenhouse, "Design of planar rectangular microelectronic inductors," *IEEE Trans. Parts, Hybrids, Packag.*, vol. PHP-10, 1974.
[8] F. W. Grover, *Inductance Calculations.* New York: Van Nostrand, 1962.
[9] F. E. Terman, *Radio Engineering Handbook.* New York: McGraw-Hill, 1943.
[10] E. Pettenpaul, H. Kapusta, A. Weisgerber, H. Mampe, J. Luginsland, and I. Wolff, "CAD models of lumped elements on GaAs up to 18 GHz," *IEEE Trans. Microwave Theory Tech.*, vol. 36, pp. 294–304, Feb. 1988.
[11] J. R Wait and K. P. Spies, "Low-frequency impedance of a circular loop over a conducting ground," *Electron Lett.*, vol. 9, no. 15, pp. 346–348, July 1973.
[12] R. E. Collin, *Foundations for Microwave Engineering*, 2nd ed. New York: McGraw-Hill, 1992, sec. 3.12.
[13] J. R. Wait, *Geo-electromagnetism.* New York: Academic, 1982, ch. 3.
[14] M. Abramowitz and I. A. Segun, *Handbook of Mathematical Functions.* New York: Dover, 1970, ch. 11.
[15] J. R. Wait, private communication, May 1996.

Samir F. Mahmoud graduated from the Electronic Engineering Department, Cairo University, Giza, Egypt, in 1964. He received the M.Sc. and Ph.D. degrees from the Electrical Engineering Department, Queen's University, Kingston, Ont., Canada, in 1970 and 1973, respectively.

During the academic year 1973–1974, he was a Visiting Research Fellow at the Cooperative Institute for Research in Environmental Sciences (CIRES), Boulder, CO. He spent two sabbatical years (1980–1982) between Queen Mary College, London, U.K., and British Aerospace, Stevenage, U.K., where he was involved in the research and design of feeds for satellite antennas. Since 1964, he has been with the staff of the Electronic Engineering Department, Cairo University, where he is a Full Professor. He is currently also a Professor at Kuwait University, Safat, Kuwait. His research activities have been in the areas of geophysical application of electromagnetic waves, communication in mine tunnel environments, satellite antennas, optical fiber communication, microwave components, and wave interaction with composite materials.

Eric Beyne received the degree in electrical engineering, and the Ph.D. degree in applied sciences, both from the University of Leuven, Leuven, Belgium, in 1983 and 1990, respectively.

From 1983 to 1985, he was a Research Assistant at the University of Leuven. In 1986, he joined IMEC, as he worked towards his Ph.D. degree on the interconnection of high-frequency digital circuits. He is presently responsible for projects on multichip modules and advanced packaging at IMEC.

Dr. Beyne is a member of the ISHM-Benelux Committee.